



This is a repository copy of *The Modelling and Control of AC Electric Winders*.

White Rose Research Online URL for this paper:  
<http://eprints.whiterose.ac.uk/77032/>

---

**Monograph:**

Zhao, R. and Edwards, J.B. (1986) *The Modelling and Control of AC Electric Winders*.  
Research Report. Acse Report 300 . Dept of Automatic Control and System Engineering.  
University of Sheffield

---

**Reuse**

Unless indicated otherwise, fulltext items are protected by copyright with all rights reserved. The copyright exception in section 29 of the Copyright, Designs and Patents Act 1988 allows the making of a single copy solely for the purpose of non-commercial research or private study within the limits of fair dealing. The publisher or other rights-holder may allow further reproduction and re-use of this version - refer to the White Rose Research Online record for this item. Where records identify the publisher as the copyright holder, users can verify any specific terms of use on the publisher's website.

**Takedown**

If you consider content in White Rose Research Online to be in breach of UK law, please notify us by emailing [eprints@whiterose.ac.uk](mailto:eprints@whiterose.ac.uk) including the URL of the record and the reason for the withdrawal request.



[eprints@whiterose.ac.uk](mailto:eprints@whiterose.ac.uk)  
<https://eprints.whiterose.ac.uk/>

Department of Control Engineering  
University of Sheffield  
Mappin Street  
SHEFFIELD  
S1 3JD

The Modelling and Control of AC Electric Winders

by

R. Zhao \*

J. B. Edwards †

A paper submitted to the IEE for consideration for publication in the Proceeding, Part B.

RESEARCH REPORT NO. 300

\* Visiting Scholar to Department of Control Engineering, University of Sheffield, and Lecturer, Automatic Control Department, Shenyang Construction Engineering College, Shenyang, China.

† Professor of Control Engineering, University of Sheffield.

October 1986

Abstract

Based on reasonable assumptions, this article establishes a set of mathematical equations for a typical electric winder system. And with a digital computer, the modelling of the closed-loop control system of the electric winder has been realised. Its operation is simple, requiring only one variable, the payload, to be input yet the operational results for the entire control system are satisfactory.

200041200



## 1. INTRODUCTION

### 1.1 The Winder Control Problem.

Mine automation is a crucial area of application for control engineering for reasons of economy and safety of production. There are many links in the transport chain between production-faces underground and the separation plant at the surface and the mine-winder, lifting mineral from great depths (100 to 5000 m), was the first of these operations to which automatic control techniques were applied. Considerable success was achieved with expensive d.c.-driven winders powered initially from Ward-Leonard motor-generators, later from mercury-arc rectifiers and more-recently from their solid-state equivalents (thyristors). These drives are nowadays capable of operating without human supervision and fully interlocked with mine-car handling systems at pit-bottom and pit-top as well as with simple skip-hoisting systems.

The 3-phase a.c. induction motor drive with rotor-resistance control, though a very popular choice for winder electrification in the mid 1960's due to its relative cheapness, has proved much more difficult to control precisely. The relationship between generated torque, motor slip and rotor resistance is highly nonlinear, the moving electrode structure of the liquid controller typically used, has a high inertia requiring a powerful servo system and complicated mechanical linkage for its adjustment and the resistance/electrode position relationship is highly nonlinear. The relationship is also time-varying because evaporation due to the large rate of energy dissipation (often 1000's KW are average) through the electrolyte causes fairly rapid changes in concentration throughout the working shift.

With manual supervision, closed-loop speed-control was accomplished with only moderate period of creep speed at the end of each wind to compensate for the above-listed factors and to accommodate the variable stretch of the winding rope (1 to 2 m) caused by payload fluctuations from wind-to-wind. With the loss of driver intelligence on moving to totally automatic systems, however,

the creep period necessary to accomplish safe winding became excessive.

No comprehensive analysis of the problem was ever published however and as progress in the automation of other mining operations (mining, underground transportation and surface preparation) proceeds, the winder problem now requires scrutiny if it is not to inhibit future productivity of the overall mine.

In this paper we therefore present an analysis, control design and simulation of the a.c. winder which incorporates most of the problems discussed above and encouraging results are reported.

### 1.2 The Winding System Investigated.

There are many kinds of electrical winder systems being adopted in the world. What is concerned in this paper is the system which includes an a.c. slip-ring motor, a reducing gear, a cylindric drum and two cages which are suspended by an elastic steel-wire rope to the drum respectively with no tail rope suspended underneath<sup>†</sup> (see Fig.1)

In this system, we suppose that loaded cage 1 is to be lifted up from pit bottom to pit top and unloaded cage 2 descended from pit top to pit bottom at the same time. The operation speed of the system is controlled by a large power rheostat (or a liquid controller) which is in series with the rotor circuit.

In the past, the change of the resistance of rotor circuit was realized by an operator who worked

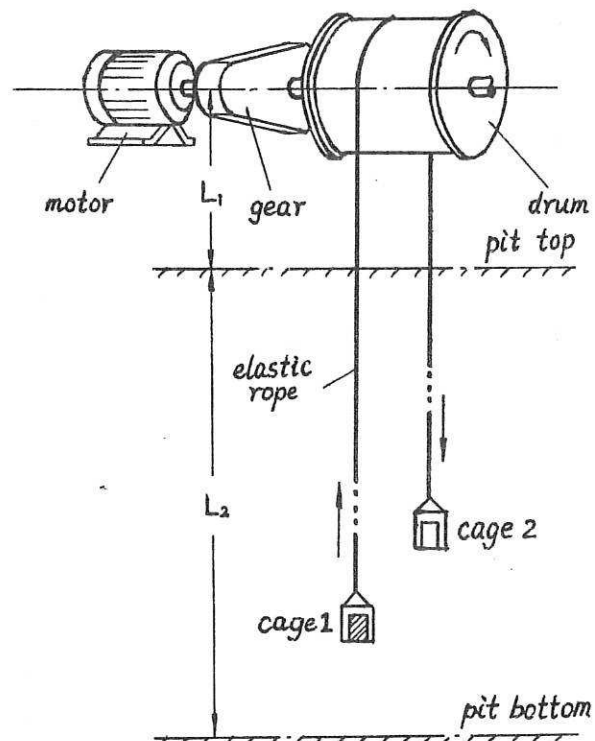


Fig.1 Schematic Diagram of the System

<sup>†</sup> A tail-rope simplifies the problem but is uncommon on drum winders.

at an operation deck. Even at present there are still a lot of this kind of system operated by man. The production efficiency and reliability of the system, of course, are depended upon the operator's skill to a large extent.

In this article we introduce a simple method to control the operation of the system. As long as the datum of payload is input into the system, both cages can be respectively driven to the assigned places accurately and smoothly in certain time.

It should be noticed that all the quantities used in this article are in engineering unit system, i.e, m-kg-s unit system.

## 2. DYNAMIC PROPERTIES OF THE SYSTEM

According to the approximate theory of a.c. induction motors, the output torque  $T_q$  of the motor can be expressed as

$$T_q = K \frac{\alpha s}{\alpha + s} \quad (1)$$

where

$$K = 0.102 \frac{V^2}{\omega_s X} \quad (2)$$

$$\alpha = \frac{R_a + R_b}{X} \quad (3)$$

$$s = \frac{\omega_s - \omega}{\omega_s} \quad (4)$$

where  $V$  is the voltage applied to the stator,  $X$  the total combined stator and rotor leakage reactance at supply frequency referred to the stator winding,

$R_a$  and  $R_b$  are the resistances of rotor coil itself and external speed-controlled circuit respectively,  $\omega_s$  the synchronous speed of the motor and  $\omega$  the actual speed of the motor.

For convenience, we use Fig.2 to represent the motion of drum-rope-cage subsystems, in which  $A_{1b}$ ,  $A_1$ ,  $A_{1e}$  and  $A_{2b}$ ,  $A_2$ ,  $A_{2e}$  represent the actual places of both cages at the beginning, some middle time and the end of motion respectively and  $B_{1b}$ ,  $B_1$ ,  $B_{1e}$  and  $B_{2b}$ ,  $B_2$ ,  $B_{2e}$  represent corresponding locations of both

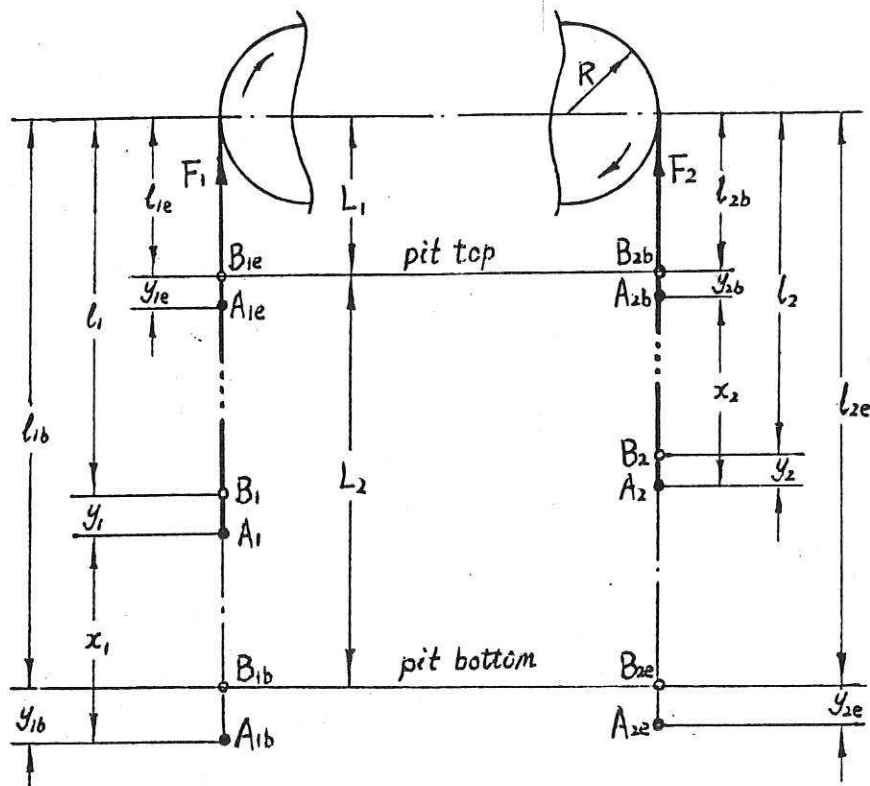


Fig.2 Schematic Diagram of Both Drum-Rope-Cage Sub-systems

cages respectively in the case without considering the elasticity of the rope. It should be noticed that  $B_{1e}$  and  $B_{2b}$  are at pit top and  $B_{1b}$  and  $B_{2e}$  at pit bottom, which will be convenient in analysing the system and make it operate repeatedly under same "initial" conditions from cycle to cycle\*. This is very important to any autocontrolled systems with repeated operations.

If the friction coefficient between the drum and rope is large enough so that there is no slip between them and the friction loss between rotating parts can be neglected and applying Newton's law of motion to the drum we obtain:

$$T_g G - F_1 R + F_2 R = \frac{I}{G} \frac{d\omega}{dt} \quad (5)$$

where  $G$  is gear ratio.,  $R$  the radius of the drum,  $I$  the total inertia of all rotating parts reduced to the drum shaft and  $F_1$  and  $F_2$  are the forces acting on the drum by the ropes suspended from it on each side.

It is evident from Fig.2 that

\* A cycle is here defined as two winds i.e. one cage passing up and down

$$F_1 = W_p + W_e + (L_1 + L_2 - \int \frac{R}{G} \omega dt) g_s + \frac{M_p + M_e + (L_1 + L_2 - \int \frac{R}{G} \omega dt) p_s}{g} \frac{R}{G} \frac{d\omega}{dt} + b \frac{R}{G} \omega \quad (6)$$

$$F_2 = W_e + (L_1 + \int \frac{R}{G} \omega dt) g_s + \frac{M_e + (L_1 + \int \frac{R}{G} \omega dt) p_s}{g} \frac{R}{G} \frac{d\omega}{dt} - b \frac{R}{G} \omega \quad (7)$$

where  $W_p$ ,  $M_p$  and  $W_e$ ,  $M_e$  are the weights and masses of payload and empty cage respectively,  $g_s$  and  $p_s$  are the rope weight and mass per unit length respectively and  $b$  is the coefficient of resistance including air resistance and friction drag between cage and sliding shoes.

Substituting  $F_1$  and  $F_2$  into (5) we get

$$\frac{d\omega}{dt} = \frac{G}{I + [2M_e + M_p + (2L_1 + L_2) p_s] R^2 / g} \{ T G - [W_p + (L_2 - 2 \int \frac{R}{G} \omega dt) g_s] R - 2b \frac{R}{G} \omega \} \quad (8)$$

$$\omega = \int \frac{d\omega}{dt} dt \quad \omega(0) = 0 \quad (9)$$

If  $y$  is the stretch of a piece of rope having free length  $l$  and acted on its end by an external force  $F$ , we can express it as follows:

$$y \approx \frac{l}{EA} (F + \frac{l}{2} g_s) \quad (10)$$

where  $E$  and  $A$  are the modulus of elasticity and section area of the rope respectively (see APPENDIX).

From Fig.2, the external force acting onto the rope on the side of cage 1 and making it stretch includes four parts, namely (a) the weight of the cage, (b) additional force when the cage is under variable motion, (c) the force making the rope with the mass of  $l_{1ps}$  change its speed and (d) resistance. According to the principle of elastic mechanics, the stretch  $y_1$  of the rope should be satisfied with the following equation

$$W_e + W_p + \frac{M_e + M_p}{g} \frac{R}{G} \frac{d\omega}{dt} + \frac{\ell_1 p_s}{g} \frac{R}{G} \frac{d\omega}{dt} + b \frac{R}{G} \omega + \frac{\ell_1}{2} g_s$$

$$= K_1 y_1 + b \dot{y}_1 + \frac{M_e + M_p + 0.5 \ell_1 p_s}{g} \ddot{y}_1$$

where  $K_1 = EA/\ell_1$ .

Noting that

$$\ell_1 = L_1 + L_2 = \int \frac{R}{G} \omega dt \quad (11)$$

$$y_1 = y_{1b} + \int \frac{R}{G} \omega dt - x_1 \quad (12)$$

$$y_{1b} = \frac{L_1 + L_2}{EA} (W_p + W_e + \frac{L_1 + L_2}{2} g_s) \quad (13)$$

we can get

$$\ddot{x}_1 = \frac{EA}{(M_p + M_e + 0.5 \ell_1 p_s) \ell_1} y_1 - \frac{b g \dot{x}_1}{M_p + M_e + 0.5 \ell_1 p_s}$$

$$- \frac{\ell_1 p_s}{2(M_p + M_e + 0.5 \ell_1 p_s)} \frac{R}{G} \frac{d\omega}{dt} - g \quad (14)$$

$$\dot{x}_1 = \ddot{x}_1 dt \quad \dot{x}_1(0) = 0 \quad (15)$$

$$x_1 = \int \dot{x}_1 dt \quad x_1(0) = 0 \quad (16)$$

Similarly we can write out the stretch equation of the rope on the side of cage 2 as follows

$$W_e - \frac{M_e}{g} \frac{R}{G} \frac{d\omega}{dt} - \frac{\ell_2 p_s}{g} \frac{R}{G} \frac{d\omega}{dt} - b \frac{R}{G} \omega + \frac{\ell_2}{2} g_s$$

$$= K_2 y_2 + b \dot{y}_2 + \frac{M_e + 0.5 \ell_2 p_s}{g} \ddot{y}_2$$

where  $K_2 = EA/\ell_2$ .

Noting that

$$\ell_2 = L_1 + \int \frac{R}{G} \omega dt \quad (17)$$

$$y_2 = y_{2b} - \int \frac{R}{G} \omega dt + x_2 \quad (18)$$

$$y_{2b} = \frac{L_1}{EA} (W_e + \frac{L_1}{2} g_s) \quad (19)$$

we obtain

$$\ddot{x}_2 = - \frac{EA g}{(M_e + 0.5 \ell_2 p_s) \ell_2} y_2 - \frac{b g \dot{x}_2}{M_e + 0.5 \ell_2 p_s} - \frac{\ell_2 p_s}{2(M_e + 0.5 \ell_2 p_s)} \frac{R}{G} \frac{d\omega}{dt} + g \quad (20)$$

$$\dot{x}_2 = \int \ddot{x}_2 dt \quad \dot{x}_2(0) = 0 \quad (21)$$

$$x_2 = \int \dot{x}_2 dt \quad x_2(0) = 0 \quad (22)$$

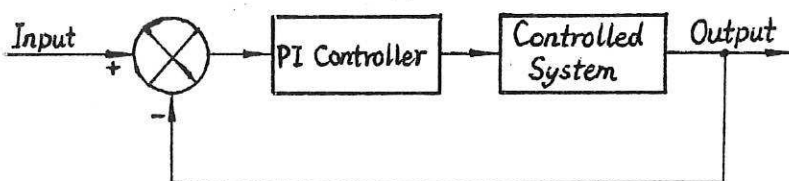
We have now derived all the equations we need to solve our system given the input functions  $V(t)$  and  $R_b(t)$  and the system constants. The design of a suitable control policy for manipulation of the system inputs is nontrivial however and is considered next in Section 3.

### 3. ESTABLISHMENT OF A CLOSED-LOOP CONTROL SYSTEM

An important problem is the choice of input variables to the whole system. We consider them as follows.

#### 3.1 Application of the PI controller.

In closed-loop control systems PI strategies remain popular despite theoretical advantages of modern alternatives. We therefore consider PI control first (Fig.3).



The output in our case is taken as the actual speed of cage 1. The input to the whole system should be, therefore, a speed-demand or

*Fig.3 Schematic Diagram of a Closed-loop Control System*

"reference speed". The error between the two speeds is input to the PI controller, which produces a signal to control the resistance  $R_b$  of the control rheostat. The transfer function of the controller can be shown as

$$\frac{O(z)}{I(z)} = K_p + \frac{K_i}{1-z^{-1}}$$

Because of the integrating action the change of the resistance cannot be made as fast as desired: the change of the actual speed of the cage always lags behind the reference speed, especially at the beginning of the operation causing a very small actual starting speed, even a negative one. To overcome this problem we connect an additional starting rheostat called  $R_c$  in series with  $R_a$  and  $R_b$  and make it linearly reduce its value during the acceleration

period. Equation (3) is, therefore, changed to:

$$\alpha = \frac{R_a + R_b + R_c}{X} \quad (23)$$

### 3.2 Voltage Applied onto Motor Stator

From equation (1) and (2) we know that the output torque is proportional to the square of the voltage applied onto the motor stator and will determine the output speed of the system with equation (14) and (15). If the reference speed is as shown in Fig.4, the voltage should be high enough in acceleration period and low enough in deceleration period, yet in the middle period should be changed accordingly under the condition

that the value of the reostat is larger than or equal to zero. The manipulation of voltage is further complicated

because the rope weights on both sides of the drum are changing throughout the operation period. If the main voltage

is fixed and there are only a stator contactor to change the direction of supply and a  $\Delta - \lambda$  convertor in the system, we can use them to produce some kinds of stepped voltage patterns according to time and the payload (see Section 4.2).

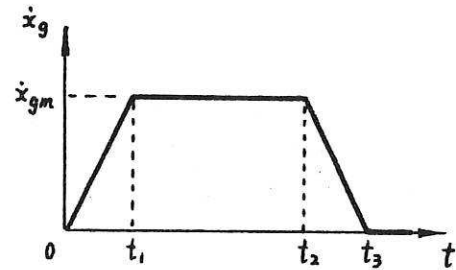


Fig. 4 A Reference Speed Curve

### 3.3 Reference Speed and Brake Patterns

If the reference speed curve shown in Fig.4 is adopted and  $t_1$ ,  $t_2$  and  $t_3$  are fixed under any conditions, the maximum value  $\dot{x}_{gm}$  of the speed should be changed with the payload so that at the end of operation cage 1 can come to rest as smoothly and steadily as possible, reducing the vibration of the cage to a great extent and, therefore, shorten the cycle time.

From experiments we have found that there are definite relations between  $\dot{x}_{gm}$  and  $W_p$  and the type of voltage pattern needed for satisfactory control of the winder. The use of these patterns certainly benefits the accuracy of computer control of the system.

Once the cage arrives at desired end position, i.e. pit top in our case, the brake should be applied so that loading and unloading operations can be effected without making further demands on the control system which can then be reset to the necessary condition for next cycle. Mechanical braking is not our concern in this article but can be assumed perfect provided the final approach speed is sufficiently small.

#### 4. COMPUTER MODELLING

##### 4.1 Parameters of a Sample System

Rated Payload $W_p$	3000 kg
Weight of Cage and Tubes $W_e$	3200 kg
Weight of Rope $g_s$	4.5 kg/m
Elastic Module of Rope $E$	$5 \times 10^9$ kg/m <sup>2</sup>
Section Area of Rope $A$	$9.5 \times 10^{-4}$ m <sup>2</sup>
Distance between Drum and Pit Top $L_1$	30 m
Lifting Distance $L_2$	300 m
Acting Radius of Drum $R$	1.5 m
Gear Ratio $G$	8.2
Motor Power $W$	375 KW
Polar Number of Stator $p$	10
Main Frequency $f$	50 Hz
Resistance of Rotor $R_a$	0.4 $\Omega$ /ph
Total Leakage Reactance $X$	5.75 $\Omega$ /ph
Total Rotating Inertia Referred to Drum Shaft $I$	7000 Kg.m.s <sup>2</sup>
Cycle length $T$	80 s
Hoisting Period $T_1$	60 s

##### 4.2 Patterns of Applied Voltage and Reference Speed

Through a series of experiments we have found that in order to achieve satisfactory results, different patterns of voltage should be applied to the stator

according to different payload. Corresponding to these, different reference speed patterns ( $\dot{x}_{gm}$ ) should be used. It can be known that under the condition that the main voltage is 3000 volts the maximum payload the system will be able to suit to is about 3400 kg. We have divided the payloads from 0 to 3400 kg into 6 sections. Their patterns of applied voltage (replaced by K - see equation (2)) and the corresponding reference speed are shown in Fig.5 and equations (24) and (25) respectively.

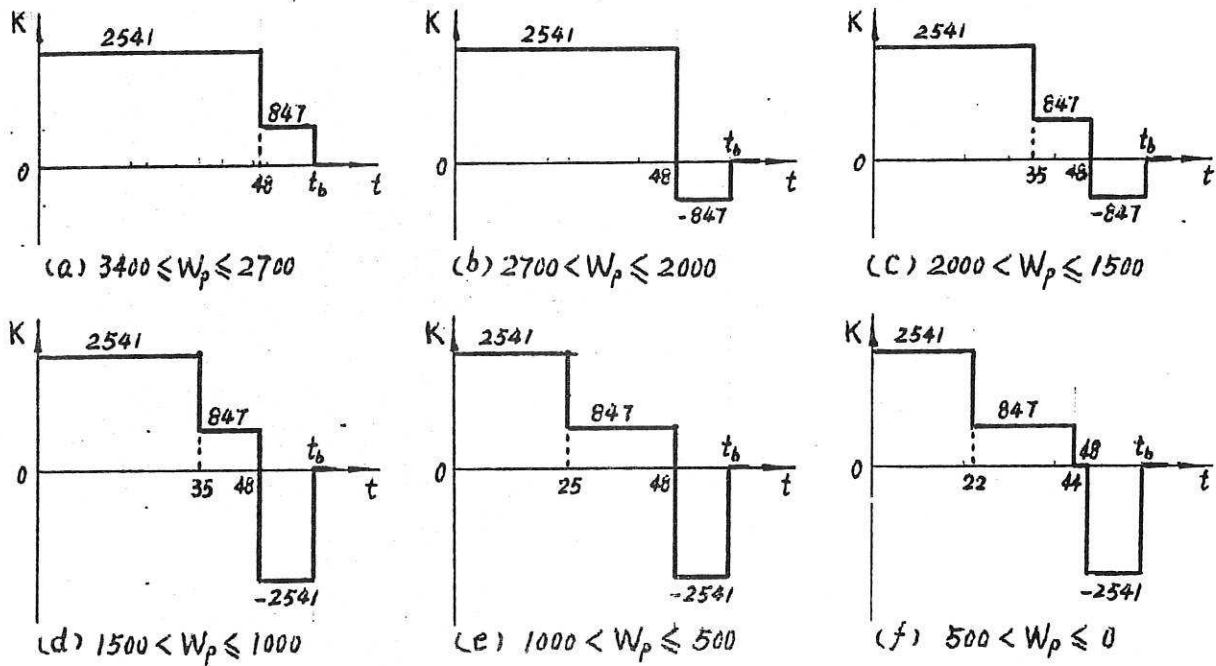


Fig. 5 Patterns of Applied Voltage

$$\dot{x}_g = \begin{cases} \left( \frac{\dot{x}_{gm}}{12} t \right) & 0 \leq t < 12 \\ \left( \dot{x}_{gm} \right) & 12 \leq t < 48 \\ \left( \frac{\dot{x}_{gm}}{12} (60-t) \right) & 48 \leq t < 60 \\ \left( 0 \right) & 60 \leq t < 80 \end{cases} \quad (24)$$

$$\dot{x}_{gm} = a_i W_p^2 + b_i W_p + c_i \quad (i = 1 \sim 6) \quad (25)$$

In equation (25),  $a_i$ ,  $b_i$ , and  $c_i$  are determined by experiments.

#### 4.3 Modelling Program and Operation Results

From the foregoing analysis and design we can now establish the program

modelling the operation of the whole system, which has only one input value, namely the payload  $W_p$ . Fig.6 is a block diagram of the program, in which the numeral in block represents the code name of the equation with which some part of the program will be executed and L is used to indicate the actual position of the cage, which, from Fig.2, is

$$L = - (L_1 + L_2 + y_{1b} - x_1) \quad (26)$$

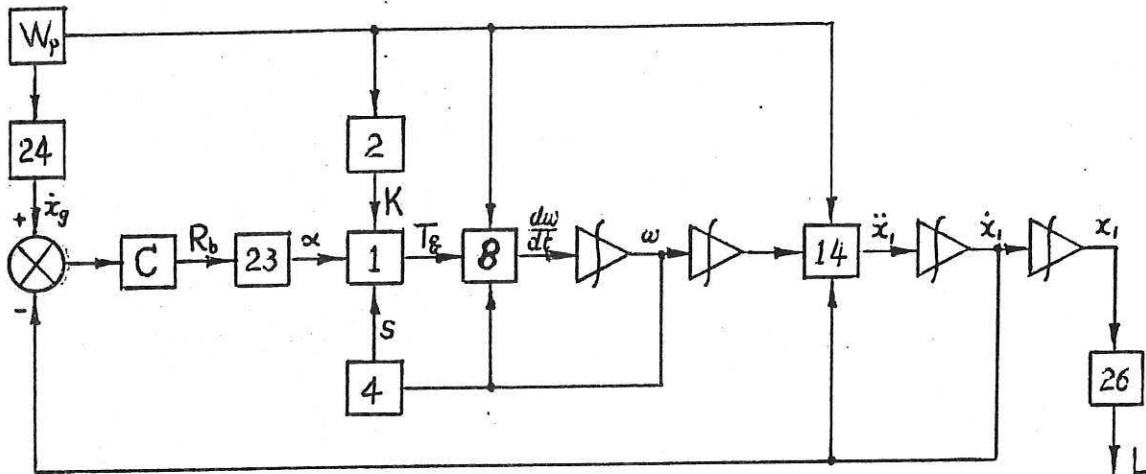


Fig.6 Block Diagram of Modelling Program

We here give typical results for the simulated operation of the system in Figs.7 to 14 and Tables 1 and 2, in which the variables are identified as follows:  $R_8$  represents  $\dot{x}_g$ ;  $I_4$   $\dot{x}_1$ ;  $RB$   $R_b$ ;  $WJ$   $L$ ;  $RF$   $K$ ;  $M4$   $T_g$ ;  $WI$   $y_1$  and  $I_5$   $x_1$ . From Figs. 8, 10, 12 and 14 we can see there is evident vibration of the stretch  $y_1$  at the beginning of operation at a frequency of about 0.5 Hz which accords clearly with the theoretical figure of 0.6 Hz. It has been important to include the rope-stretch dynamics because vibration can sometimes greatly upset the performance of nonlinear machine/control system of this type. The control system we propose in this paper clearly performs well despite the vibration which is reassuring for its future implementation. Rope stretch, however, does not seriously affect the landing accuracy of the loaded cage at the pit top since (as shown in the APPENDIX) the stretch is given by

$$y_{1e} = \frac{L_1}{EA} (W_p + \frac{L_1}{2} g_s)$$

and  $L_1$  is very small at the pit top. If  $W_p$  is 3000 Kg, for example, then  $y_{1e}$  is only 0.019 m. (From Table 1,  $y_{1e} = 0.016$  m can be obtained. The difference between the two values for  $y_{1e}$  is due only to calculation error).

The control error with this system is the discrepancy between the desired cycle time (i.e. the time to execute the trapezoidal speed reference pattern) and the actual time for the winder to come to rest. (There is no discernable distance error between landing position and pit top with this system). An interesting feature of the proposed system is that the time error varies between negative and positive values with changing payload (e.g. - 2.5 seconds with 1000 kg payload and +2.5 seconds with 3000 kg payload). It should therefore be possible to minimise the average time discrepancy in practice by carefully mutating the controlled parameters to the particular winding system involved.

## 5. CONCLUSIONS

The purpose of this article is inquiring into a better technique to realize the closed-loop control of electrical winder system. From Figs. 7 to 14 and Table 1 and 2 we can see that the operation results are satisfactory if only the payload is within the range from 0 to 3400 kg. But, on the other hand, since the voltage applied to the stator cannot be changed continuously and smoothly when only a  $\Delta - \lambda$  convertor and a stator contactor are used in the system, the actual speed of the cage cannot change very smoothly. There are some kinds of techniques to solve this problem, which, for example, are using thyristors and reverse system to produce continuously changeable a.c. voltage and applying a tail rope to cage bottoms. We are not going to discuss these problems here.

## 6. REFERENCES

- (1) Broughton H.H., "ELECTRIC WINDERS" 2nd Ed. E & F.N. Spon, London, 1948.  
pp 22 - 35.

- (2) Statham I.C.F, "COAL MINING PRACTICE" Vol.II, Caxton, London, 1958.  
p.295.
- (3) Cannon R.H, "DYNAMICS OF PHYSICAL SYSTEMS" McGraw-Hill, U.S.A. 1967,  
pp 244-299.
- (4) Say M.G, "ALTERNATING CURRENT MACHINES" 5th ed. Pitman, London, 1983, p254.

7. APPENDIX

For analysing the stretch of the rope we turn to Fig.15 in which  $\ell$  represents the free length of the rope and  $y$  is its stretch under the action of external force  $F$  plus its own weight. Suppose the rope is even everywhere and dividing  $\ell$  into  $n$  sections each having same length  $\Delta\ell$ , then from the top end to the bottom-end of the rope, the stretches of these sections of the rope  $\Delta y_1, \Delta y_2, \dots, \Delta y_n$  are as follows:

$$\begin{aligned} \Delta y_1 &= \frac{\Delta\ell}{EA} (F + \frac{n-1}{n} \ell g_s) + B \\ \Delta y_2 &= \frac{\Delta\ell}{EA} (F + \frac{n-2}{n} \ell g_s) + B \\ &\vdots \\ \Delta y_{n-1} &= \frac{\Delta\ell}{EA} (F + \frac{1}{n} \ell g_s) + B \\ \Delta y_n &= \frac{\Delta\ell}{EA} F + B \end{aligned}$$

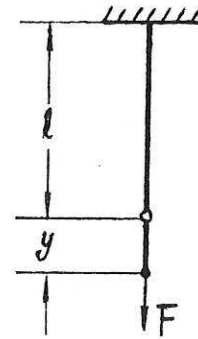


Fig. 15 Stretch of Elastic Rope

where  $E$  represents the modulus of elasticity of the rope,  $A$  its section area and  $B$  the stretch produced by the weight of the piece of the rope being considered. Thus we can obtain

$$y = \sum_{i=1}^n \Delta y_i = \frac{\ell}{EA} (F + \frac{\ell}{2} g_s - \frac{\Delta\ell}{2} g_s) + nB \quad (7.1)$$

If we divide  $\Delta\ell$  further into  $m$  pieces each having same length  $\Delta\ell'$ , then the stretches of these pieces  $\Delta y'_1, \Delta y'_2, \dots, \Delta y'_m$  produced by the rope weight itself will be

$$\begin{aligned}\Delta y'_1 &= \frac{\Delta \ell'}{EA} \frac{m-1}{m} \Delta \ell g_s + C \\ \Delta y'_2 &= \frac{\Delta \ell'}{EA} \frac{m-2}{m} \Delta \ell g_s + C \\ &\vdots \\ \Delta y'_{m-1} &= \frac{\Delta \ell'}{EA} \frac{1}{m} \Delta \ell g_s + C \\ \Delta y'_m &= C\end{aligned}$$

where C represents the stretch produced by the weight of the smaller piece of the rope  $\Delta \ell'$  being considered.

Adding all the m equations together we get

$$B = \sum_{j=1}^m \Delta y'_j = \frac{\Delta \ell'}{EA} \left( \frac{\Delta \ell}{2} g_s - \frac{\Delta \ell'}{2} g_s \right) + m C$$

Substituting B into (7.1) we obtain

$$y = \frac{\ell}{EA} \left( F + \frac{\ell}{2} g_s - \frac{\Delta \ell'}{2} g_s \right) + m n C \quad (7.2)$$

Since  $\Delta \ell'$  is the second-order small quantity and C is the third one, we can rewrite (7.2) as

$$y \approx \frac{\ell}{EA} \left( F + \frac{\ell}{2} g_s \right) \quad (7.3)$$

Equation (7.3) shows that the stretch of an even rope with considering its own weight is equal to that of the rope without weight on its own but with half of its weight suspended at its lower end.

-RK4- DT= 0.10 M<sub>p</sub>=3000kg  
 MEMORY 1 (A) MEMORY 2 (B) MEMORY 3 (C) MEMORY 4 (D)  
 RB 10. I4 10. RB 10. WJ 0.00

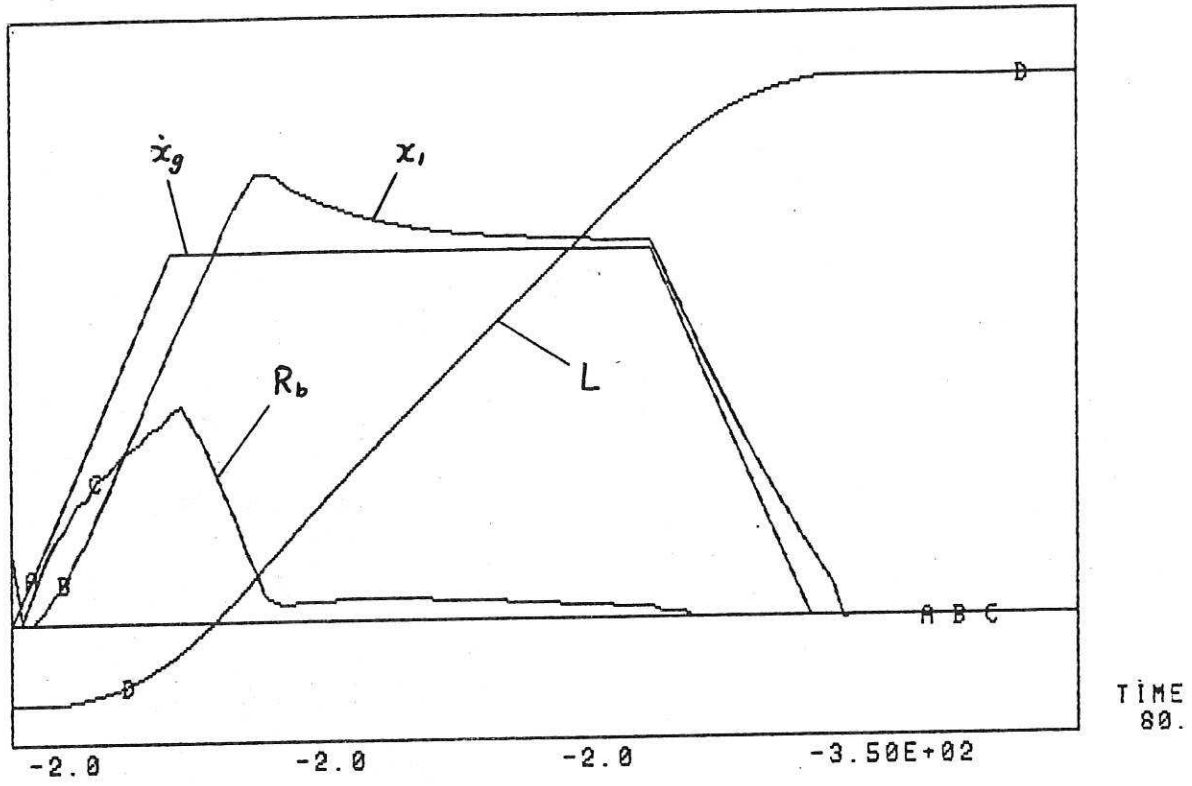


Fig. 7 Operation Results 1 With  $W_p = 3000$  kg

-RK4- DT= 0.10 M<sub>p</sub>=3000kg  
 MEMORY 1 (A) MEMORY 2 (B) MEMORY 3 (C) MEMORY 4 (D)  
 RF 3.00E+03 M4 1.50E+03 WI 0.55 I5 3.10E+02

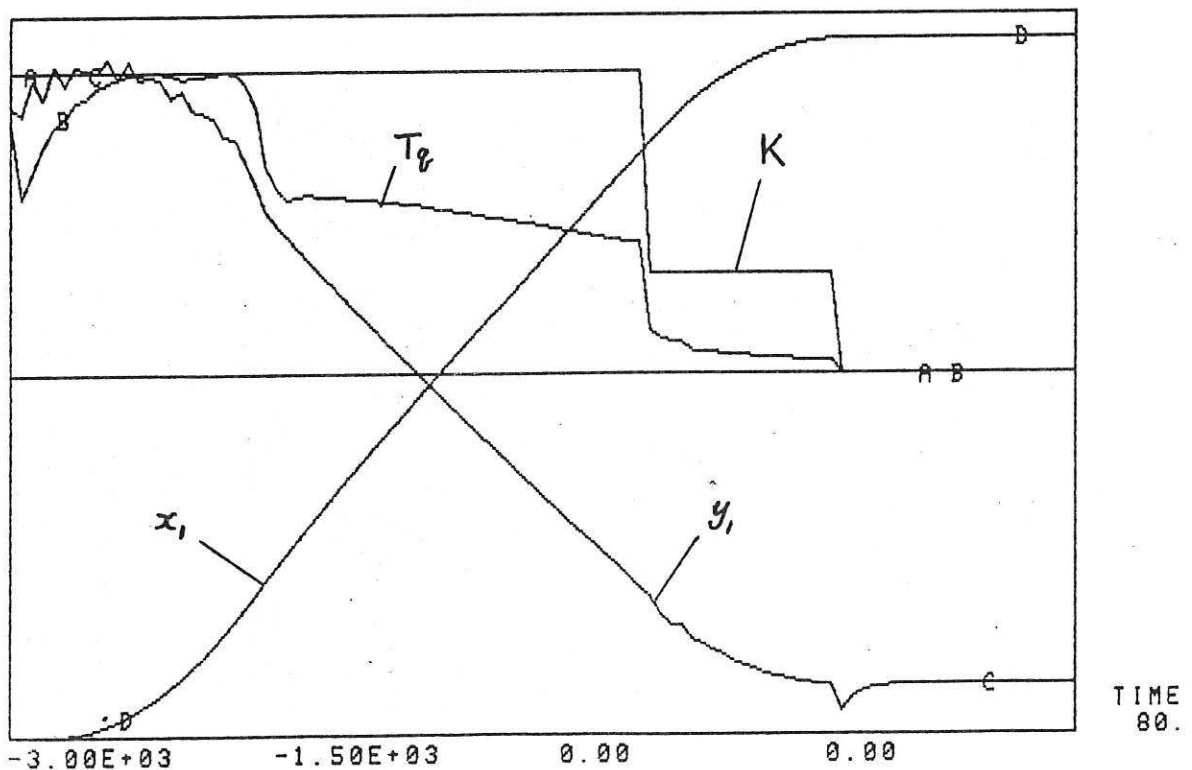


Fig. 8 Operation Results 2 With  $W_p = 3000$  kg

Table 1. Operation Results 1 With  $W_p = 3000$  kg

TIME	RB	I 4	RB	WJ
0.000	0.000000	0.000000	1.2000	-330.48
2.40	1.2326	0.21915	1.0029	-330.34
4.00	2.0544	0.70569	1.6179	-329.59
6.40	3.2870	1.8422	2.4193	-326.58
8.00	4.1088	2.6025	2.7341	-323.06
10.4	5.3414	3.8626	3.2222	-315.36
12.0	6.1632	4.6435	3.5180	-308.58
14.4	6.1632	5.7723	3.0028	-296.14
16.0	6.1632	6.5133	2.1930	-286.33
18.4	6.1632	7.4503	0.81438	-269.46
20.0	6.1632	7.3812	0.31203	-257.55
22.4	6.1632	7.0479	0.33842	-240.28
24.0	6.1632	6.8935	0.34982	-229.13
26.4	6.1632	6.7193	0.36629	-212.81
28.0	6.1632	6.6316	0.36845	-202.13
30.4	6.1632	6.5304	0.36178	-186.34
32.0	6.1632	6.4805	0.35278	-175.93
34.4	6.1632	6.4217	0.33527	-160.45
36.0	6.1632	6.3927	0.32113	-150.20
38.4	6.1632	6.3587	0.29740	-134.90
40.0	6.1632	6.3404	0.28032	-124.74
42.4	6.1632	6.3186	0.25341	-109.54
44.0	6.1632	6.3074	0.23342	-99.432
46.4	6.1632	6.2955	0.20667	-84.315
48.0	6.1621	6.2884	0.20048	-74.252
50.4	4.9294	5.1375	0.13099	-60.550
52.0	4.1076	4.3494	0.00000	-52.944
54.4	2.8749	3.2865	0.00000	-43.782
56.0	2.0531	2.6119	0.00000	-39.067
58.4	0.82040	1.6922	0.00000	-33.917
60.0	0.00000	1.1132	0.00000	-31.678
62.4	0.00000	-1.48729E-02	0.00000	-29.996
64.0	0.00000	2.28047E-02	0.00000	-30.011
66.4	0.00000	6.58805E-03	0.00000	-30.016
68.0	0.00000	7.26442E-03	0.00000	-30.016
70.4	0.00000	6.62922E-03	0.00000	-30.016
72.0	0.00000	7.21858E-03	0.00000	-30.016
74.4	0.00000	8.60048E-03	0.00000	-30.016
76.0	0.00000	7.16030E-03	0.00000	-30.016
78.4	0.00000	6.49897E-03	0.00000	-30.016
80.0	0.00000	7.11071E-03	0.00000	-30.016

Table 2. Operation Results 2 With  $W_p = 3000$  kg

Run:  $M_p = 3000$  kg  
 Print interval: 0.80                      0.80                      0.80                      0.80

TIME	RF	M4	W1	I5
0.000	2541.0	1061.4	0.48232	0.00000
2.40	2541.0	967.14	0.48707	0.14325
4.00	2541.0	1084.6	0.49844	0.89181
6.40	2541.0	1208.0	0.50759	3.9816
8.00	2541.0	1244.8	0.50282	7.4189
10.4	2541.0	1270.5	0.50450	15.121
12.0	2541.0	1259.7	0.48816	21.901
14.4	2541.0	1252.8	0.47739	34.347
16.0	2541.0	1269.6	0.45860	44.156
18.4	2541.0	1118.3	0.42151	61.023
20.0	2541.0	782.22	0.38969	72.936
22.4	2541.0	758.73	0.36310	90.201
24.0	2541.0	747.46	0.34537	101.35
26.4	2541.0	738.18	0.31934	117.68
28.0	2541.0	728.99	0.30232	128.35
30.4	2541.0	711.71	0.27742	144.14
32.0	2541.0	698.84	0.26109	154.55
34.4	2541.0	678.60	0.23698	170.03
36.0	2541.0	664.31	0.22108	180.28
38.4	2541.0	641.91	0.19759	195.58
40.0	2541.0	626.45	0.18214	205.75
42.4	2541.0	602.69	0.15948	220.94
44.0	2541.0	585.07	0.14478	231.05
46.4	2541.0	560.88	0.12146	246.17
48.0	847.00	185.18	0.10669	256.23
50.4	847.00	137.58	8.47168E-02	269.93
52.0	847.00	93.786	7.12091E-02	277.54
54.4	847.00	81.688	5.68848E-02	286.70
56.0	847.00	75.658	5.10254E-02	291.42
58.4	847.00	68.607	4.44336E-02	296.57
60.0	847.00	64.858	4.07715E-02	298.80
62.4	0.00000	0.00000	1.95313E-02	300.49
64.0	0.00000	0.00000	3.49121E-02	300.47
66.4	0.00000	0.00000	3.93066E-02	300.47
68.0	0.00000	0.00000	3.97949E-02	300.47
70.4	0.00000	0.00000	3.97949E-02	300.47
72.0	0.00000	0.00000	3.97949E-02	300.47
74.4	0.00000	0.00000	3.97949E-02	300.47
76.0	0.00000	0.00000	3.97949E-02	300.47
78.4	0.00000	0.00000	3.97949E-02	300.47
80.0	0.00000	0.00000	3.97949E-02	300.47

-RK4- DT= 0.10 M<sub>p</sub>=2000kg  
 MEMORY 1 MEMORY 2 MEMORY 3 MEMORY 4  
 R8 (A) I4 (B) RB (C) WJ (D)  
 10. 10. 10. 0.00

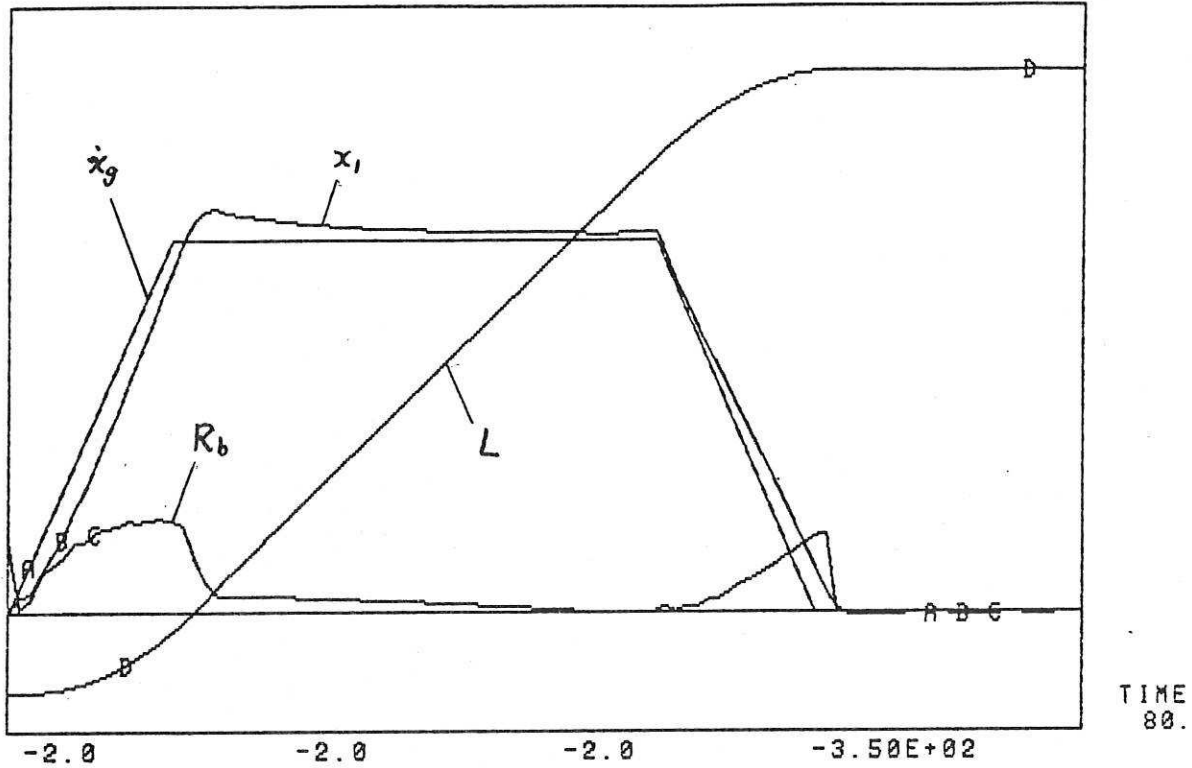


Fig.9 Operation Results 1 With W<sub>p</sub> = 2000 kg

-RK4- DT= 0.10 M<sub>p</sub>=2000kg  
 MEMORY 1 MEMORY 2 MEMORY 3 MEMORY 4  
 RF (A) M4 (B) WI (C) I5 (D)  
 3.00E+03 1.50E+03 0.55 3.10E+02

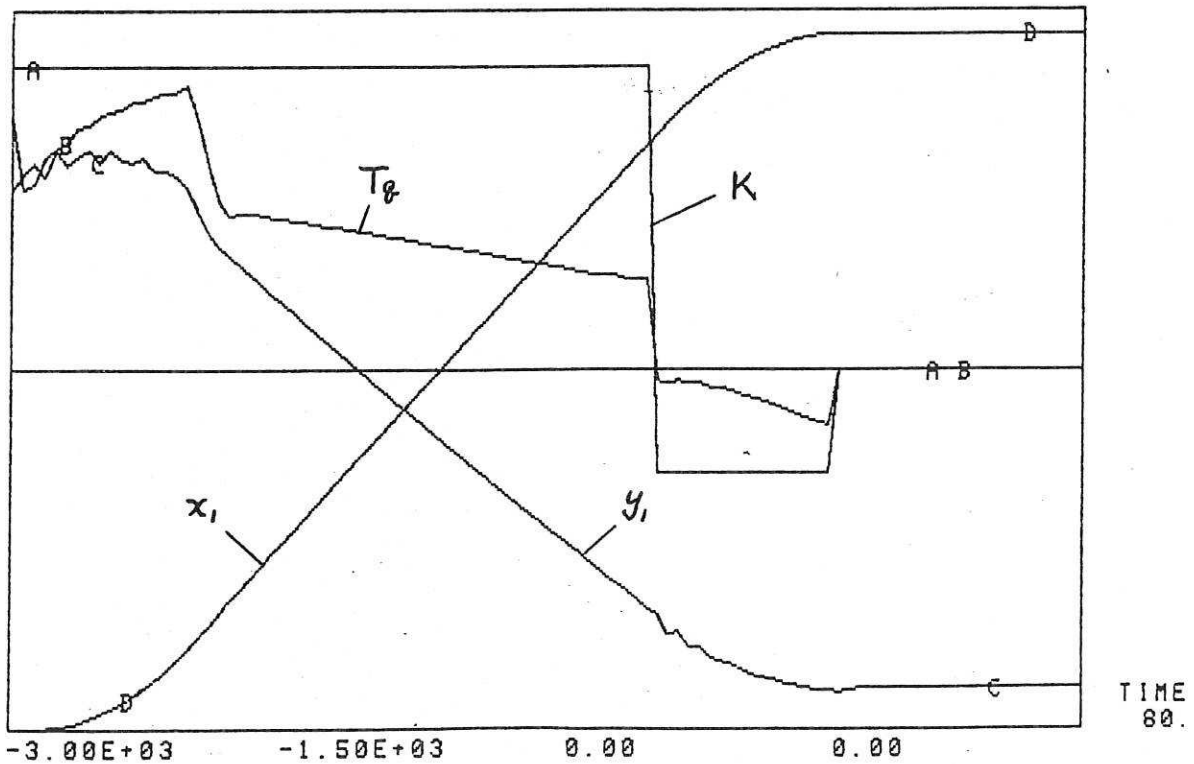


Fig.10 Operation Results 2 With W<sub>p</sub> = 2000 kg

-RK4- DT= 0.10 M<sub>p</sub>=1000kg  
 MEMORY 1 (A) MEMORY 2 (B) MEMORY 3 (C) MEMORY 4 (D)  
 RB 10. 14 10. RB 10. WJ 0.00

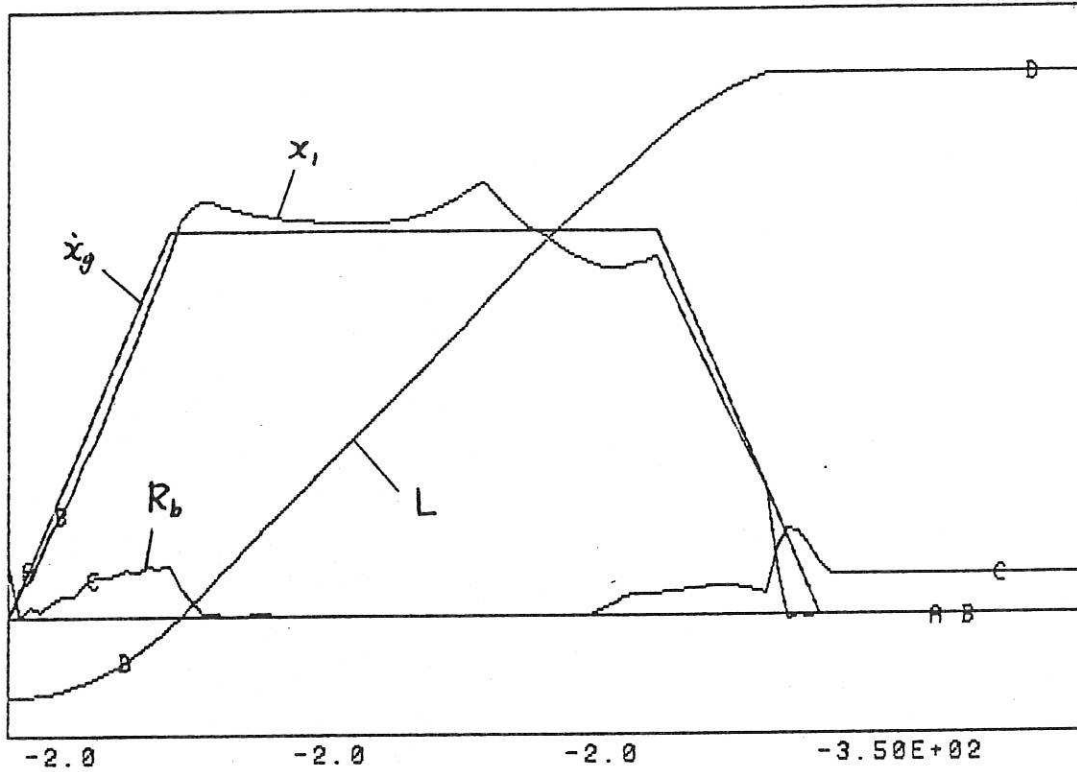


Fig. 11 Operation Results 1 With  $W_p = 1000$  kg

-RK4- DT= 0.10 M<sub>p</sub>=1000kg  
 MEMORY 1 (A) MEMORY 2 (B) MEMORY 3 (C) MEMORY 4 (D)  
 RF 3.00E+03 M4 1.50E+03 WI 0.55 IS 3.10E+02

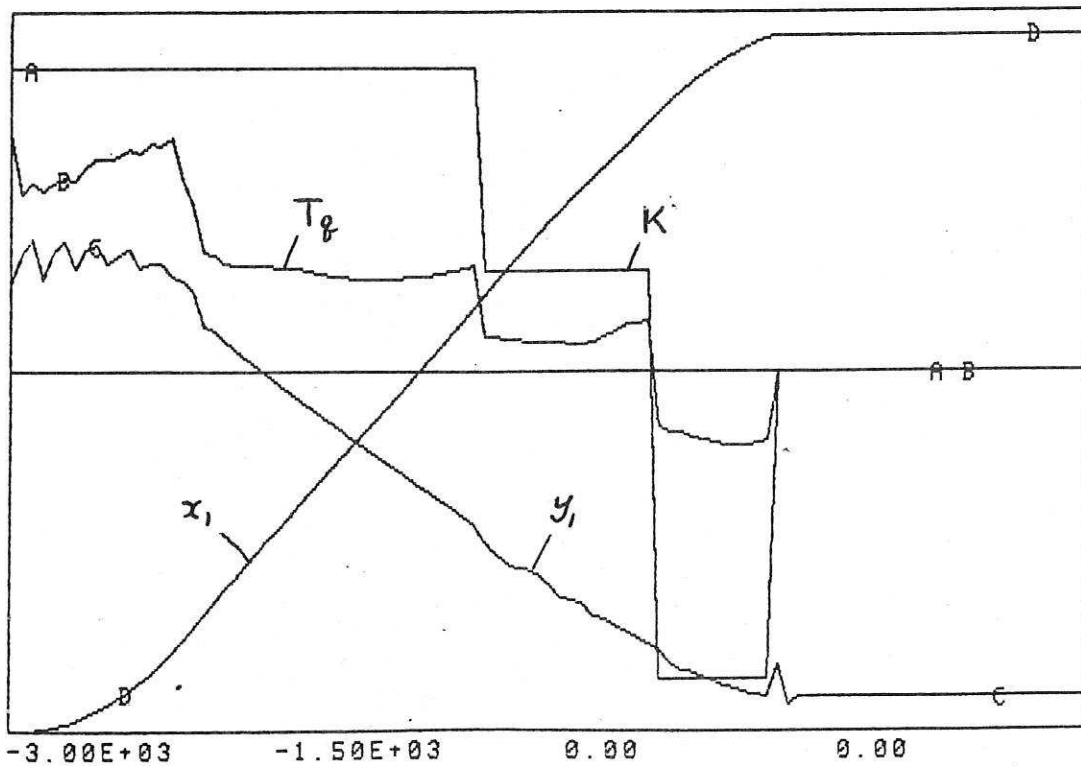


Fig. 12 Operation Results 2 With  $W_p = 1000$  kg

-RK4- DT= 0.10  $M_p=0\text{kg}$   
 MEMORY 1 (A) MEMORY 2 (B) MEMORY 3 (C) MEMORY 4 (D)  
 RB 10. I4 10. RB. 10. WJ 0.00

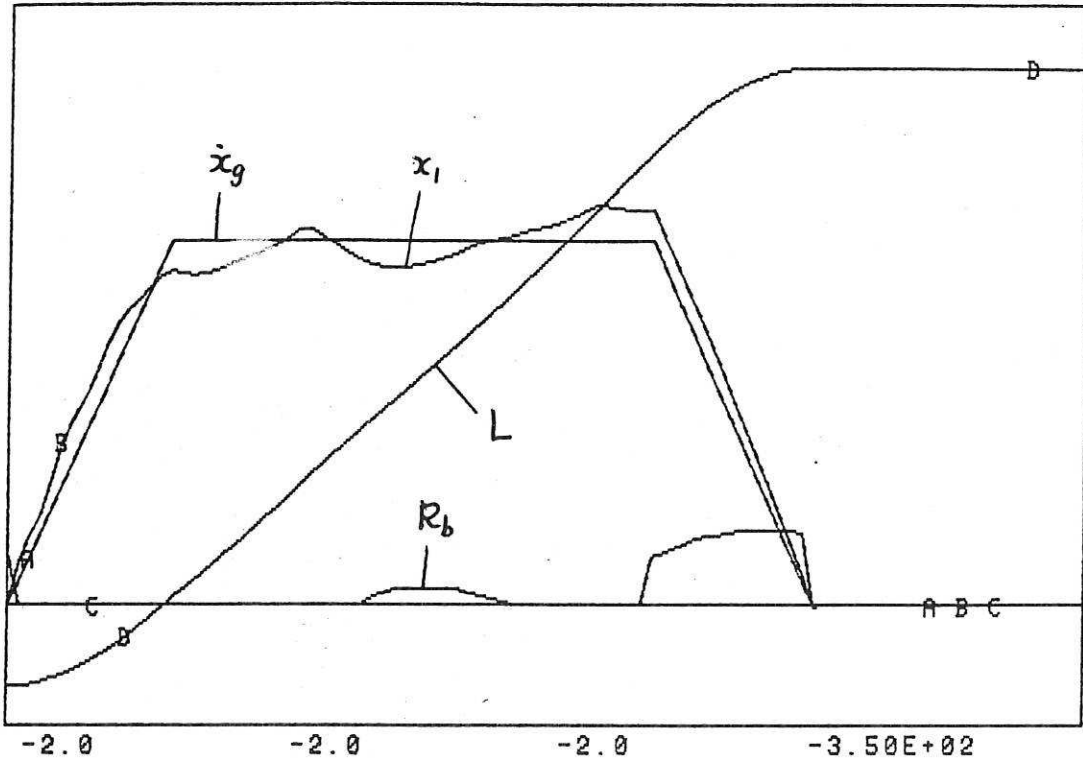
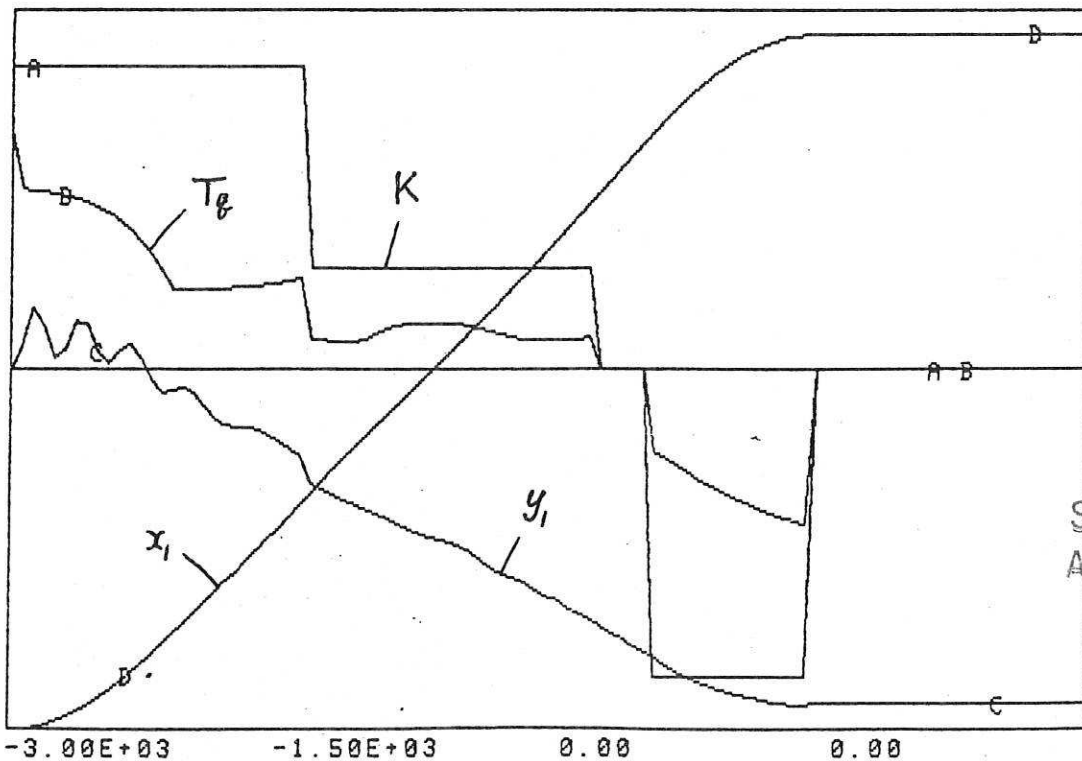


Fig.13 Operation Results 1 With  $W_p = 0\text{ kg}$

-RK4- DT= 0.10  $M_p=0\text{kg}$   
 MEMORY 1 (A) MEMORY 2 (B) MEMORY 3 (C) MEMORY 4 (D)  
 RF  $3.00E+03$  M4  $1.50E+03$  WI 0.55 I5  $3.10E+02$



SHEFFIELD UNIV.  
 APPLIED SCIENCE  
 LIBRARY.

TIME  
 80.

Fig.14 Operation Results 2 With  $W_p = 0\text{ kg}$